Quo vadis niobium? Divergent coordination behavior of early-transition metals towards MOF-5†

Maciej D. Korzyński, [ID] [a] Luca Braglia, [ID] [b] Elisa Borfecchia, [ID] [cd]
Kirill A. Lomachenko, [ID] [e] Amgalanbaatar Baldansuren, [ID] [f]
Christopher H. Hendon, [ID] [g] Carlo Lamberti [ID] ‡[hi] and Mircea Dincă [ID] *[a]

Treatment of MOF-5 with $NbCl_4(THF)_2$ in acetonitrile leads to incorporation of Nb(IV) centers in a fashion that diverges from the established cation metathesis reactivity of this iconic material. A combination of X-ray absorption spectroscopy analysis and reactivity studies altogether supported by density functional theory computational studies document an unprecedented binding mode for the $Zn_4O(O_2C-)_6$ secondary building units (SBUs), which in Nb(IV)-MOF-5 function as κ^2-chelating ligands for $NbCl_4$ moieties, with no exchange of Zn^{2+} observed. This unusual reactivity expands the portfolio of post-synthetic modification techniques available for MOFs, exemplified here by MOF-5, and underscores the diverse coordination environments offered by this and potentially other MOFs towards heterometal species.

Introduction

Nominally, the compositional variety of metal–organic frameworks (MOFs) is unlimited, with virtually any stable metal in the periodic table potentially serving as the basis for the inorganic building blocks, or the secondary building units (SBUs).[1–9] Yet, the vast majority of SBUs are made from a very limited set of metal species, nearly all MOFs featuring first-row transition metals, with heavy representation among the late first row metals. Although early transition metal (ETM)-based MOFs have distinguished themselves with remarkable stability, especially

under aqueous conditions,[10] MOFs made from ETMs are still rare outside of Zr and Ti. One of the major challenges associated with *de novo* synthesis of ETM-based MOFs is the tendency of metal precursors to undergo deleterious oxygen-scavenging reactivity under solvothermal conditions encountered in typical MOF syntheses.[11]

With an eye towards enriching the compositional space of MOFs with other ETMs and to explore the fundamentals of bonding for ETMs within this set of materials, we turned our attention to niobium, which remains essentially unexplored in this sense. Indeed, to our knowledge, there are only two reported Nb-containing frameworks in the literature.[12,13] With its flexible coordination sphere, large covalent radius, and extreme oxophilicity, niobium is the epitome of a difficult substrate for MOF formation and should therefore provide insight into the behavior of other early transition metals for this purpose.[14]

To circumvent the expected challenges associated with the direct synthesis of Nb MOFs (*vide supra*), we decided to focus on post-synthetic modification (PSM), a method that has previously proven successful in altering the chemical structure of pre-formed MOFs.[15–17] Because PSM allows for mild reaction conditions, contrasting with the harsh solvothermal synthetic routes encountered in *de novo* MOF preparation, it can lead to the isolation of materials that are difficult to form otherwise.[18] In particular, within the context of post-synthetic cation exchange[19] our group and others have shown, initially through the iconic $Zn_4O(BDC)_3$ (MOF-5; BDC = terephthalate) (Fig. 1a), that the SBUs within MOFs can be thought of as supramolecular chelating ligands for incoming metal ions. The exchanged SBUs behave spectroscopically and chemically as isolated molecules with unusual coordination environments that are often

[a]*Department of Chemistry, Massachusetts Institute of Technology, 77 Massachusetts Avenue, Cambridge, MA 02139, USA. E-mail: mdinca@mit.edu*

[b]*CNR-Istituto Officina dei Materiali, TASC Laboratory in Area Science Park - Basovizza, Strada Statale 14 km 163.5, 34149 Trieste, Italy*

[c]*Department of Chemistry, NIS, CrisDi, INSTM Centre of Reference, University of Turin, Via Quarello 15, I-10135 Torino, Italy*

[d]*Center for Materials Science and Nanotechnology (SMN), Department of Chemistry, University of Oslo, 1033 Blindern, 0315 Oslo, Norway*

[e]*European Synchrotron Radiation Facility, 71 Avenue des Martyrs, CS 40220, 38043 Grenoble Cedex 9, France*

[f]*EPSRC National EPR Facility, School of Chemistry, The University of Manchester, Oxford Road, Manchester M13 9PL, UK*

[g]*Materials Science Institute, Department of Chemistry and Biochemistry, University of Oregon, Eugene, Oregon 97403, USA*

[h]*Department of Physics, NIS, CrisDi, Interdepartmental Centers, INSTM Centre of Reference, University of Turin, Via Giuria 1, I-10125 Torino, Italy*

[i]*The Smart Materials Research Institute, Southern Federal University, 178/24 Sladkova Street, Rostov-on-Don, 344090, Russia*

† Electronic supplementary information (ESI) available. See DOI: 10.1039/c9sc01553a
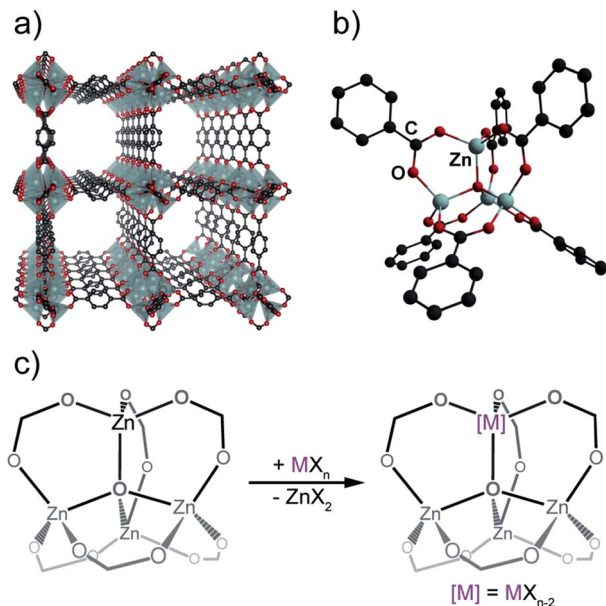
‡ Deceased February 1, 2019.

Fig. 1 (a) Structure of MOF-5, (b) its SBU, and (c) idealized cation exchange process. Hydrogen atoms were omitted for clarity.

unknown from traditional solution chemistry.[20] These earlier studies showed that the $[Zn_4O]^{6+}$ SBU (Fig. 1b) is particularly prone to exchanging Zn^{2+} for the majority of the first row transition metal cations in various oxidation states (Fig. 1c).[21–23] MOF was therefore identified as a promising platform for exploring Nb chemistry. Herein, we document our quest in understanding niobium immobilization in MOF-5, and we unveil an unprecedented coordination mode within its SBU.

Results and discussion

Appropriate starting materials are available for Nb in several oxidation states, with the Nb(IV) d^1 system offering an additional characterization handle in the form of electron paramagnetic resonance (EPR) spectroscopy, when compared to the more common Nb(V) oxidation state. To this end, the soluble niobium(IV) chloride tetrahydrofuran complex $(NbCl_4(THF)_2)$ serves as a good entry point to Nb(IV) chemistry.[24] The routine method to introduce a foreign metal into a framework involves soaking the MOF crystals in a solution of the desired precursor. Here, treatment of pre-activated, colorless MOF-5 crystals[25] with a yellow-green solution of $NbCl_4(THF)_2$ in acetonitrile (MeCN) led to an almost instantaneous change of color for the crystals to dark violet (Fig. S1†). The observed fast kinetics of this process were surprising given that reported first row cation exchange processes proceed rather slowly. After 48 h, the isolated dark violet crystals of Nb(IV)-treated MOF-5 were washed extensively with MeCN then dichloromethane (DCM) until no characteristic features of Nb(IV) could be observed in the UV spectrum of the effluent solutions. Residual solvent molecules within the pores and/or weakly-bound to the metal centers, were removed by heating to 150 °C under high vacuum (0.1 mTorr).

Powder X-ray diffraction (PXRD) analysis confirmed that treatment of MOF-5 with the niobium solution and subsequent thermal treatment proceed with preservation of crystallinity (Fig. S2†). The R_1 (9.7°-to-6.8°) and R_2 (13.8°-to-6.8°) peak ratios[26,27] were low indicating no pore obstruction by the guest molecules and lack of framework interpenetration. Inspection of the attenuated total reflection Fourier-transform infrared (ATR-FTIR) spectrum of the activated material showed predominantly typical MOF-5 features (Fig. S3†). Additional FTIR bands in the spectrum of Nb(IV)-treated MOF-5, which are absent in the spectrum of MOF-5 itself, are also present in the vacuum-dried residue obtained from a solution of $NbCl_4(THF)_2$ in acetonitrile (Fig. S4†). In particular, a prominent feature at 2282 cm^{-1} in this latter residue suggests that excess acetonitrile partially replaces THF in the primary coordination sphere of Nb(IV), in agreement with the literature data on MeCN adducts of Nb(IV),[28] and is likely carried over upon reaction with MOF-5. Importantly, this band does not persist in fully activated Nb(IV)-MOF-5, indicating full removal of MeCN from this material.

The documented tendency of Nb(IV) compounds to disproportionate thermally[29] required confirmation that niobium immobilization within MOF-5 occurs with preservation of the +IV oxidation state, which came from EPR spectroscopy and X-ray
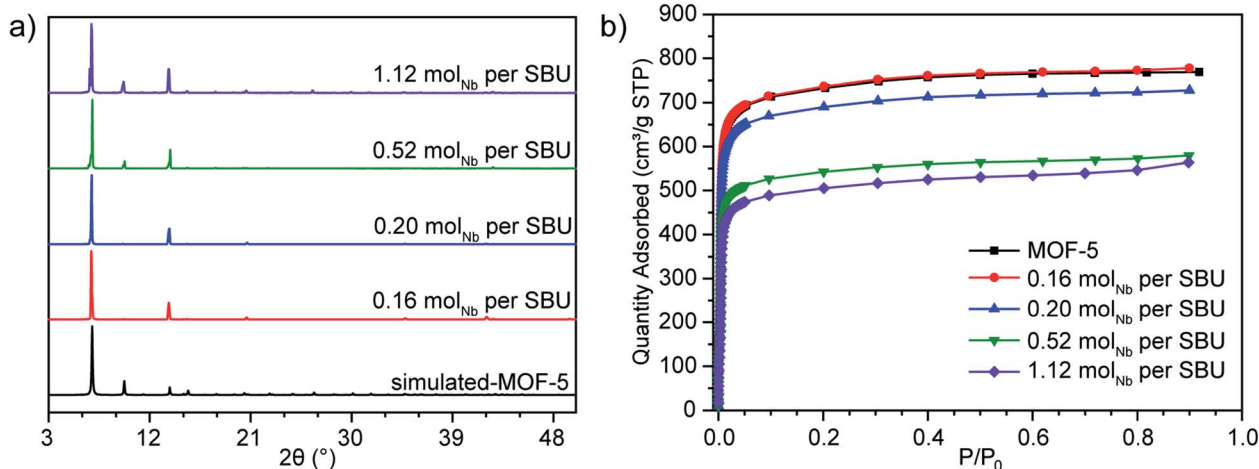

Fig. 2 (a) PXRD patterns and (b) N$_2$ adsorption isotherms for Nb(IV)-treated MOF-5 samples with increasing niobium content.

absorption spectroscopy (XAS). Although the typical hyperfine splitting pattern for ^{93}Nb (I = 9/2) is observed in the EPR spectrum of Nb(IV)-MOF-5 at X-band, the peaks are significantly broadened, with a first-order hyperfine splitting (A_{Nb}) of approximately 557 MHz (Fig. 3, Table S1†). In the simulated spectrum (Fig. S5 and S6†), the hyperfine interactions of both isotopes ^{35}Cl and ^{37}Cl (both I = 3/2 nuclei) are included, and although they do not affect the alignment of the electron spins, these contribute to inhomogeneous line broadening. Notably, EPR signals obtained for Nb(IV)-MOF-5 and a toluene-MeCN frozen glass of NbCl$_4$(-THF)$_2$ are similar, the aforementioned line broadening in the MOF notwithstanding (Fig. S7†). Finally, analysis of the XAS data in the Nb K-edge X-ray absorption near edge structure region (XANES) for Nb(IV)-treated MOF-5 and a series of Nb(IV) standards[30] confirmed that the edge energy, $\approx$19 001 eV, was in line with that of niobium(IV) oxide (Fig. S8†). These results offer confidence that Nb(IV) does not disproportionate and remains in its original oxidation state when immobilized within MOF-5.

The impact of immobilized Nb content on the properties of the MOF was probed by preparing samples containing different Nb-to-SBU molar ratios (0.16, 0.20, 0.52, and 1.12; determined by inductively coupled plasma – atomic emission spectroscopy, ICP-AES). Even when using less than one equivalent of Nb precursor with respect to the [Zn$_4$O]$^{6+}$ SBU, Nb uptake into the MOF progressed rapidly and in a qualitatively similar manner, with retention of crystallinity (Fig. 2a). This stands in contrast with cation exchange, which occurs typically only in an excess of incoming metal species and often leads to loss of crystallinity when exchange is rapid.

The porosity of the Nb(IV)-treated samples was further confirmed by N$_2$ adsorption isotherms at 77 K (Fig. 2b). Fitting these to the Brunauer–Emmett–Teller (BET) equation gave apparent surface areas ranging from 2943 m^2 g^{-1} to 2010 m^2 g^{-1} for Nb(IV)-MOF-5 samples with 0.16 mol Nb per SBU and 1.12 mol Nb per SBU, respectively. Although these are lower than anticipated for cation-exchanged materials, the decreased porosity was not caused by surface deposition of certain species that would

block access to the pores. Indeed, scanning electron microscopy – energy dispersive X-ray spectroscopy mapping revealed that niobium deposition occurs not only on the surface, but also homogeneously throughout the crystal (Fig. S9 and S10†).

With solid evidence that Nb is immobilized inside the pores of MOF-5, but with conflicting evidence regarding its substitution of Zn^{2+} ions inside the SBU, the primary coordination environment of Nb(IV) within MOF-5 was probed by XAS.[31] These studies were aided by density functional theory (DFT) calculations that modelled three Nb(IV) bonding scenarios. The first model assumed that typical cation exchange occurred, with a [NbCl$_2$]$^{2+}$ unit replacing a Zn^{2+} ion to produce a neutral Cl$_2$-NbZn$_3$O(O$_2$C–)$_6$ cluster (Fig. 4a). As shown with Ni^{2+}-exchanged MOF-5,[21] the SBU in this material is able to support octahedral metal ions, as would be required for the Nb center in this model. A second model assumed that the [Zn$_4$O]$^{6+}$ constitution of the node is preserved and that instead of exchanging any Zn^{2+} ions, a NbCl$_4$ moiety binds to the SBU in an exogenous κ^2-fashion utilizing two carboxylate oxygen atoms as anchor points (Fig. 4b). Finally, to account for the possibility of adventitious oxygen or water scavenging during the deposition, we also considered a niobyl unit (NbOCl$_2$) bound to the SBU exogenously in a κ^2-fashion similar to the NbCl$_4$ model (Fig. 4c).

The XAS data coupled with these DFT models was sufficient to discriminate the local Nb environment within MOF-5. Extended X-ray absorption fine structure (EXAFS) analysis of the XAS data for a wide range of Nb[30] allowed adoption of a two-step refinement strategy to analyze the experimental EXAFS spectrum of Nb(IV)-MOF-5: (i) in a first step, all the parameters for the three DFT-structures were optimized (Table S2†) apart from the S_0^2, which was fixed to 1 and the Debye–Waller factor of O, σ_O^2, and of Cl, σ_{Cl}^2, which were fixed from the EXAFS results obtained on the reference samples; (ii) the second step involved refinement of S_0^2 (Table S3†). Unexpectedly, the first step revealed that the fit for 'NbCl$_4$' matched the experimental data much better than other models. Confirming that no hydrolysis at the Nb center occurs, the fit for the 'NbOCl$_2$' model yielded a meaningless value of ΔE (15 ± 31) eV and an unphysically high σ^2 (0.14 ± 0.12) Å^2 for the scattering paths involving C and O atoms at distances larger than 3.2 Å from the Nb absorber. Although the parameters obtained for the 'NbCl$_2$' cation exchange model were also reasonable, the fit for this model did not match the experimental curves as well as the 'NbCl$_4$' fit. Indeed, the R-factor for the 'NbCl$_2$' model was seven times larger than that for 'NbCl$_4$' (Table S2†).

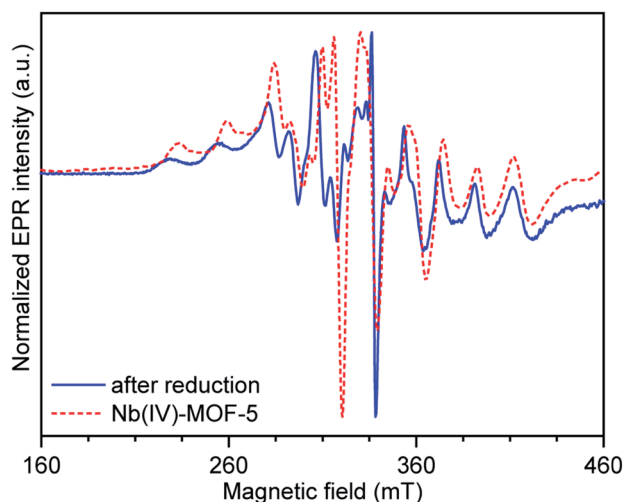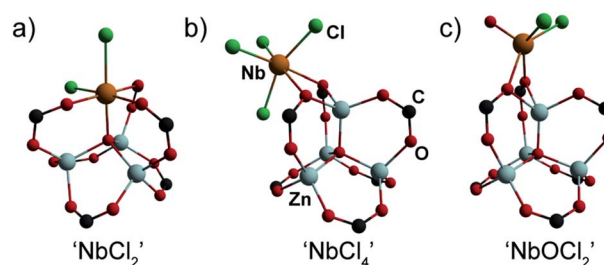**Fig. 3** EPR spectra of Nb(IV)-MOF-5 and of Nb(V)-MOF-5 treated with (TMS)$_2$pyr.

Fig. 4 DFT-optimized models of plausible Nb coordination modes in MOF-5.

The second step in the EXAFS fitting routine (Table S3†) definitely disqualified the cation exchanged ('NbCl$_2$') model as a likely candidate for Nb(IV)-MOF-5. Indeed, optimizing the S_0^2 for all three models excluded 'NbCl$_2$' both on the basis of an unreasonably high value for the energy shift ($\Delta E = 10 \pm 2$ eV) and a value that was too low for the S_0^2 parameter (0.51 ± 0.04). Lastly, the best qualitative agreement between the fit and experimental curves was obtained for the 'NbCl$_4$' model (Fig. 5, red curves), which we therefore favor as the dominant coordination environment of Nb in Nb(IV)-MOF-5. The final fit parameters for this model (Fig. S11†) gave Nb–O distances of 2.49(5) Å and two independent sets of Cl atoms situated at 2.23(4) Å and 2.41(2) Å from the niobium center.

Immobilization of hetero-metal species in MOF-5 by means other than cation exchange has received little attention in the literature. In fact, the vast majority of examples that employ decoration of the SBUs with exogenous metals, rather than cation exchange, are reported for Zr-based materials.[16,32–35] One recent example with transition metals in MOF-5 involved the installation of Fe(OH)$_3$(H$_2$O)$_2$ moieties bridging SBUs on two interpenetrated lattices,[36] with limited additional examples focusing on alkali metal decoration of MOF-5.[37–42] These findings point to a previously unrecognized divergence in the reactivity of early and late transition metals with oxygen-based SBUs: whereas the late transition metals favor cation exchange reactivity (the Zr-based MOFs notwithstanding[43]), we show here that the high-valent early transition metals prefer to adhere to the SBU rather than exchange within the SBU, presumably because of their extreme oxophilicity. Notably, MOF-5 is a rare instance that allows both processes to occur.§ Further proof of exogenous SBU binding of Nb(IV), rather than exchange within the SBU, came from a clean reaction between Nb(IV)-MOF-5 and XeF$_2$ in MeCN, which caused a swift color change of the violet crystals to off-white and emergence of a yellow solution. Inspection of the off-white solid by ICP-AES showed that niobium was almost quantitatively removed from the material, with preservation of crystallinity (Fig. S12†). This would be unlikely if niobium served a structural role as part of the SBU.

Immobilization of early transition metal ions by decoration of the MOF-5 SBU can be extended to Nb(V), which furthermore engages in molecule-like, well behaved redox chemistry within the MOF, reminiscent of the behavior of late transition metals in the same material. Thus, soaking MOF-5 in a solution of NbCl$_5$ in MeCN yielded Nb(V)-MOF-5 as an off-white crystalline powder. Despite the higher Lewis acidity[44] and even higher oxophilicity of Nb(V) relative to Nb(IV), Nb(V)-decorated MOF-5 also retains crystallinity (Fig. S14†) and, upon activation in a similar manner to the Nb(IV) MOF, shows porosity with a BET surface area of 1437 m^2 g^{-1} (Fig. S16†). This value is lower than that of Nb(IV)-MOF-5, as may be expected for a material with an additional chloride protruding into the pore. A testament to the molecule-like, site-isolated environment of Nb(V) within this material was its clean reduction with 2,3,5,6-tetramethyl-1,4-bis(trimethylsilyl)-1,4-diaza-2,5-cyclohexadiene ((TMS)$_2$pyr), a practical reagent for the reduction of high-valent early transition metal halides.[45] Treatment of Nb(V)-MOF-5 with an excess of (TMS)$_2$pyr in THF led to rapid change of color of the solids from off-white to dark blue, a transformation that once again occurred with preservation of crystallinity (Fig. S17†). The reduced MOF exhibited an X-band EPR spectrum in THF that was qualitatively similar to that of independently-synthesized Nb(IV)-MOF-5 obtained from NbCl$_4$(THF)$_2$ (Fig. 3, blue trace). Although a simple inner-sphere electron transfer reaction, this transformation demonstrates that metal centers decorating the MOF-5 SBU are amenable for further synthetic elaboration in a manner similar to those exchanged *into* the SBU.

Conclusions

In our endeavors to advance the niobium chemistry in MOFs, we discovered a novel coordination mode of foreign metal species to the SBU of MOF-5. Our results show that it is possible both to introduce and to remove niobium ions with the preservation of the parent framework's crystallinity. The chemical competence of these extra framework Nb sites is exemplified by simple reduction of Nb(V) to Nb(IV) within the framework. Excitingly, literally 20 years after its initial discovery, MOF-5, arguably one of the most iconic materials in its class, continues to surprise. This bodes well for the richness of fundamental chemistry yet to be discovered with the other thousands of MOFs out there.

Conflicts of interest

There are no conflicts to declare.

Acknowledgements
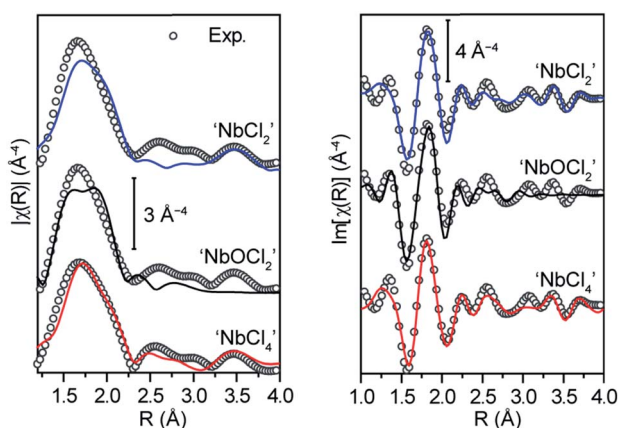
Fig. 5 Comparison of EXAFS fits for various models of Nb moieties within MOF-5.

Notes and references

§ Even though it has been reported that SBUs undergo cation exchange in the UiO-66 framework, it was later shown that deposition of the foreign metal oxide was instead occurring, see ref. 43.

1 J.-R. Li, J. Sculley and H.-C. Zhou, *Chem. Rev.*, 2012, **112**, 869–932.

2 H. Li, K. Wang, Y. Sun, C. T. Lollar, J. Li and H.-C. Zhou, *Mater. Today*, 2018, **21**, 108–121.

3 L. E. Kreno, K. Leong, O. K. Farha, M. Allendorf, R. P. Van Duyne and J. T. Hupp, *Chem. Rev.*, 2012, **112**, 1105–1125.

4 F.-Y. Yi, D. Chen, M.-K. Wu, L. Han and H.-L. Jiang, *Chempluschem*, 2016, **81**, 675–690.

5 W. P. Lustig, S. Mukherjee, N. D. Rudd, A. V. Desai, J. Li and S. K. Ghosh, *Chem. Soc. Rev.*, 2017, **46**, 3242–3285.

6 D. Farrusseng, S. Aguado and C. Pinel, *Angew. Chem., Int. Ed.*, 2009, **48**, 7502–7513.

7 C. A. Downes and S. C. Marinescu, *ChemSusChem*, 2017, **10**, 4374–4392.

8 N. S. Bobbitt, M. L. Mendonca, A. J. Howarth, T. Islamoglu, J. T. Hupp, O. K. Farha and R. Q. Snurr, *Chem. Soc. Rev.*, 2017, **46**, 3357–3385.

9 J.-S. Qin, S. Yuan, C. Lollar, J. Pang, A. Alsalme and H.-C. Zhou, *Chem. Commun.*, 2018, **54**, 4231–4249.

10 S. Yuan, L. Feng, K. Wang, J. Pang, M. Bosch, C. Lollar, Y. Sun, J. Qin, X. Yang, P. Zhang, Q. Wang, L. Zou, Y. Zhang, L. Zhang, Y. Fang, J. Li and H.-C. Zhou, *Adv. Mater.*, 2018, **30**, 1704303.

11 T. Devic and C. Serre, *Chem. Soc. Rev.*, 2014, **43**, 6097–6115.

12 A. Cadiau, K. Adil, P. M. Bhatt, Y. Belmabkhout and M. Eddaoudi, *Science*, 2016, **353**, 137–140.

13 S. Ahn, N. E. Thornburg, Z. Li, T. C. Wang, L. C. Gallington, K. W. Chapman, J. M. Notestein, J. T. Hupp and O. K. Farha, *Inorg. Chem.*, 2016, **55**, 11954–11961.

14 L. G. Hubert-Pfalzgraf, *Niobium & Tantalum: Inorganic & Coordination Chemistry in Encyclopedia of Inorganic Chemistry*, ed. R. A. Scott, John Wiley & Sons, Ltd, 2006.

15 K. K. Tanabe and S. M. Cohen, *Chem. Soc. Rev.*, 2011, **40**, 498–519.

16 R. J. Marshall and R. S. Forgan, *Eur. J. Inorg. Chem.*, 2016, **2016**, 4310–4331.

17 Z. Yin, S. Wan, J. Yang, M. Kurmoo and M.-H. Zeng, *Coord. Chem. Rev.*, 2019, **378**, 500–512.

18 N. Stock and S. Biswas, *Chem. Rev.*, 2012, **112**, 933–969.

19 C. K. Brozek and M. Dincǎ, *Chem. Soc. Rev.*, 2014, **43**, 5456–5467.

20 H. Li, M. Eddaoudi, M. O'Keeffe and O. M. Yaghi, *Nature*, 1999, **402**, 276–279.

21 C. K. Brozek and M. Dincǎ, *Chem. Sci.*, 2012, **3**, 2110.

22 C. K. Brozek and M. Dincǎ, *J. Am. Chem. Soc.*, 2013, **135**, 12886–12891.

23 C. K. Brozek, V. K. Michaelis, T.-C. Ong, L. Bellarosa, N. López, R. G. Griffin and M. Dincǎ, *ACS Cent. Sci.*, 2015, **1**, 252–260.

24 J. W. Herndon, Niobium(IV) Chloride in Encyclopedia of Reagents for Organic Synthesis, John Wiley & Sons, Ltd, 2001.

25 S. S. Kaye, A. Dailly, O. M. Yaghi and J. R. Long, *J. Am. Chem. Soc.*, 2007, **129**, 14176–14177.

26 B. Chen, X. Wang, Q. Zhang, X. Xi, J. Cai, H. Qi, S. Shi, J. Wang, D. Yuan and M. Fang, *J. Mater. Chem.*, 2010, **20**, 3758.

27 J. Hafizovic, M. Bjørgen, U. Olsbye, P. D. C. Dietzel, S. Bordiga, C. Prestipino, C. Lamberti and K. P. Lillerud, *J. Am. Chem. Soc.*, 2007, **129**, 3612–3620.

28 T. A. Dougherty, PhD thesis, Iowa State University, 1967.

29 R. E. McCarley and B. A. Torp, *Inorg. Chem.*, 1963, **2**, 540–546.

30 M. D. Korzyński, L. Braglia, E. Borfecchia, C. Lamberti and M. Dincǎ, *Inorg. Chem.*, 2018, **57**, 13998–14004.

31 S. Bordiga, E. Groppo, G. Agostini, J. A. van Bokhoven and C. Lamberti, *Chem. Rev.*, 2013, **113**, 1736–1850.

32 K. Manna, P. Ji, Z. Lin, F. X. Greene, A. Urban, N. C. Thacker and W. Lin, *Nat. Commun.*, 2016, **7**, 12610.

33 S. Yuan, L. Zou, H. Li, Y.-P. Chen, J. Qin, Q. Zhang, W. Lu, M. B. Hall and H.-C. Zhou, *Angew. Chem., Int. Ed.*, 2016, **55**, 10776–10780.

34 Z. Li, A. W. Peters, V. Bernales, M. A. Ortuño, N. M. Schweitzer, M. R. DeStefano, L. C. Gallington, A. E. Platero-Prats, K. W. Chapman, C. J. Cramer, L. Gagliardi, J. T. Hupp and O. K. Farha, *ACS Cent. Sci.*, 2017, **3**, 31–38.

35 M. D. Korzyński, D. F. Consoli, S. Zhang, Y. Román-Leshkov and M. Dincǎ, *J. Am. Chem. Soc.*, 2018, **140**, 6956–6960.

36 R. J. Holmberg, T. Burns, S. M. Greer, L. Kobera, S. A. Stoian, I. Korobkov, S. Hill, D. L. Bryce, T. K. Woo and M. Murugesu, *Chem.–Eur. J.*, 2016, **22**, 7711–7715.

37 A. Blomqvist, C. M. Araujo, P. Srepusharawoot and R. Ahuja, *Proc. Natl. Acad. Sci. U. S. A.*, 2007, **104**, 20173–20176.

38 S. S. Han and W. A. Goddard, *J. Am. Chem. Soc.*, 2007, **129**, 8422–8423.

39 S. J. Kolmann, B. Chan and M. J. T. Jordan, *Chem. Phys. Lett.*, 2008, **467**, 126–130.

40 M. Dixit, T. A. Maark and S. Pal, *Int. J. Hydrogen Energy*, 2011, **36**, 10816–10827.

41 N. T. T. Ha, O. V. Lefedova and N. N. Ha, *Russ. J. Phys. Chem. A*, 2016, **90**, 220–225.

42 S. Chaemchuem, Z. Kui and F. Verpoort, *CrystEngComm*, 2016, **18**, 7614–7619.

43 M. S. Denny, L. R. Parent, J. P. Patterson, S. K. Meena, H. Pham, P. Abellan, Q. M. Ramasse, F. Paesani, N. C. Gianneschi and S. M. Cohen, *J. Am. Chem. Soc.*, 2018, **140**, 1348–1357.

44 C. Z. Andrade, *Curr. Org. Synth.*, 2004, **1**, 333–353.

45 T. Saito, H. Nishiyama, H. Tanahashi, K. Kawakita, H. Tsurugi and K. Mashima, *J. Am. Chem. Soc.*, 2014, **136**, 5161–5170.

46 O. Mathon, A. Beteva, J. Borrel, D. Bugnazet, S. Gatla, R. Hino, I. Kantor, T. Mairs, M. Munoz, S. Pasternak, F. Perrin and S. Pascarelli, *J. Synchrotron Radiat.*, 2015, **22**, 1548–1554.